CHEMICAL ENGINEERING TRANSACTIONS
VOL. 32, 2013
A publication of AIDIC
The Italian Association of Chemical Engineering
Online at: www.aidic.it/cet
Chief Editors: Sauro Pierucci, Jiří J. Klemeš

ISBN 978-88-95608-23-5; **ISSN** 1974-9791
DOI: 10.3303/CET1332058

Electrodeposition and Photo-electrochemical Behaviour of CIGS Thin Films and Nanowire Arrays for Solar Cell

Rosalinda Inguanta*, Tiziana Spanò, Roberto L. Oliveri, Salvatore Piazza, Carmelo Sunseri

Laboratorio di Chimica Fisica Applicata, Dipartimento di Ingegneria Chimica Gestionale Informatica Meccanica, Università di Palermo, Viale delle Scienze, 90128 Palermo (Italy)
rosalinda.inguanta@unipa.it

In this work, we present some results concerning the electrochemical fabrication of CIGS thin films and nanowires, for semiconducting p-n junction fabrication. Tuned nanowire length and composition were achieved by adjusting applied potential and electrolyte composition. Also in the case of thin films, composition was controlled by varying the concentration of metal salts in the electrodeposition bath. Deposits were characterized by X-ray diffraction (XRD), Scanning Electrode Microscopy (SEM), Raman Spectroscopy, Energy Dispersion Spectroscopy (EDS) and by photo-electrochemical measurements. XRD patterns showed that as-synthesized semiconducting compounds were amorphous, independent of deposition conditions. EDS analysis revealed the formation of CIGS compounds with different values of the Cu/(In+Ga) and Ga/(In+Ga) ratios. In order to tune the composition of CIGS, thermal treatment at ~400 °C for 1h was also performed under Ar atmosphere. Photoelectrochemical measurements showed that CIGS compounds display cathodic photocurrent independent of deposition conditions, whilst different optical gap values were measured.

1. Introduction

In the field of solar energy conversion there is an increasing interest toward semiconducting compounds of copper, indium, gallium ad selenium (CIGS) as absorber layer, due to their high absorption coefficient (~10^5 cm^{-1}), tunable band gap (from ~1 to ~1.7 eV) and long-term opto-electronic stability (Panthani 2008). The greatest advantages of CIGS technology are the minimal amount of material required and the high cell efficiencies compared to other thin film technologies. In fact, crystalline cells are about 200 μm thick, while the CIGS absorber is less than 2 μm thick. Besides, more than half of this layer consists of relatively inexpensive copper. Another significant advantage of this technology is the possibility to deposit directly the thin semiconductor layer and the contacts on a substrate that can be of different nature, like glass, aluminium or plastic. In particular, with two last supports it is possible to fabricate flexible solar cell, ideal for installation on curved surfaces and/or structurally weak supports, but also for their possible use as a power source in mobile devices.
The highest-efficiency solar cell (20.3%), was recently obtained in Centre for Solar Energy and Hydrogen Research (ZSW) (Jackson et al, 2011) and it was fabricated using a $CuInGaSe_2$ film deposited by a modified co-evaporation process. Manz Automation (www.manz.com) has produced the new world highest module efficiency with polycrystalline CIGS (14.6%), close to that of polycrystalline silicon solar modules, but with significantly lower costs. Despite these good results, many studies are in progress up to date in order to increase the efficiency of CIGS solar cells and to develop new processes that should be cheap, easily scalable and environmentally compatible. For this aim, an interesting approach is to use a single-step electrochemical deposition as fabrication method, which is a low cost technique, easy scalable to high electrode area and it is a process environmentally compatible owing to the use of simple aqueous solutions. Moreover by electrodeposition it is possible to obtain CIGS in nanostructured shapes that improve solar cell performance.

Please cite this article as: Inguanta R., Spano T., Oliveri L., Piazza S., Sunseri C., 2013, Electrodeposition and photo-electrochemical behavior of cigs thin films and nanowire arrays for solar cell, Chemical Engineering Transactions, 32, 343-348 DOI: 10.3303/CET1332058

In this work we have explored the electrodeposition technique in order to optimize this process for the deposition of CIGS thin films and nanostructures. Thin films were electrodeposited on electropolished molybdenum sheets, whilst nanostructures were obtained by template electrodeposition into pores of an anodic alumina membrane. Aim of the work is to adjust the composition of electrolytic bath in order to have, after thermal treatment, a deposit with a stoichiometry close to $Cu_{0.23}In_{0.18}Ga_{0.085}Se_{0.505}$, which is the optimal composition according to the researchers of NREL laboratory, (Basol, 2010).
Results concerning deposits chemical composition, before and after annealing, together with the response under monochromatic illumination, will be presented and discussed.

2. Experimental

Thin films were deposited on electropolished Mo sheets whilst nanostructures were grown inside the channels of anodic alumina membrane by a single-step potentiostatic deposition, at room temperature under N_2 atmosphere, and from electrolytes consisting of metal sulphates mixtures. For depositions on Mo sheet substrates, a specific electropolishing pre-treatment, described in (Spanò et al. 2013), was adopted. This treatment is necessary to remove the oxide layer and to obtain a defect-free smooth Mo surface. In the case of anodic alumina membrane, prior to deposition, a thin film of gold was sputtered onto one surface of the membrane in order to make it conductive. A detailed description of electrode fabrication is reported in our previous works (Inguanta et. al, 2007, 2009, 2010a, 2010b). For both substrates, active sample area was delimited by means of an insulating lacquer. Electrochemical experiments were performed using a PAR potentiostat/galvanostat (PARSTAT, mod. 2273). Depositions were carried out potentiostatically under nitrogen atmosphere in a three-electrode cell having a Pt mesh as the counter-electrode and a saturated calomel as the reference electrode (SCE, E°=+0.24 V/NHE), using aqueous solutions of metal sulphate salts with different concentrations and at room temperature. During depositions, current vs. time curves were monitored and acquired through POWERSUITE™ software.
Samples morphology was analyzed through scanning electron microscopy (SEM), using a FEI FEG-ESEM (mod. QUANTA 200) equipped with an Energy Disperse Spectroscopy (EDS) detector. Samples were also characterized by XRD analysis, using an ItalStructures (APD2000) diffractometer, having a Cu Kα radiation (λ = 0.154 nm) as the source, with a step of 0.02 degrees and a measuring time of 0.5 s for each step. XRD peaks were identified by comparison with the ICDD Database. Raman spectroscopy was performed using a Renishaw, inVia Raman Microscope, equipped with a He-Ne laser beam having a spot size of 2 μm and calibrated by means of the Raman peak of a polycrystalline Si (520 cm^{-1}).
Photoelectrochemical measurements were carried out in a 0.1 M Na_2SO_4 solution (pH=5.6) at room temperature, using a cell having flat quartz windows for allowing sample illumination. A three electrodes system was employed, with a platinum wire as counter electrode and a mercury sulphate (MSE, E°=+0.66 V/NHE) as reference. Monochromatic irradiation was achieved using a 150 W Xe lamp (Oriel) coupled to a UV/visible monochromator (Baush & Lomb). For improving resolution, photocurrent was detected by a two-phase lock-in (EG & G, mod. 5206), connected to a mechanical chopper (frequency: 10 Hz). To suppress second harmonic response, a yellow filter was inserted in the light path before recording photocurrents at long wavelengths. Data were acquired by a desk computer through an analogic interface using a LABVIEW™ 7 software and processed according to home-written programs. Photocurrent spectra reported below are corrected for the photon emission of the lamp/monochromator system at each wavelength; the latter was detected previously using a calibrated thermopile (Newport).
Samples were characterized before and after thermal treatment, performed at ~400 °C for 1h under Ar atmosphere.

3. Results and Discussion

Simultaneous electrodeposition of Cu, In, Ga and Se is very challenging, because it involves four elements having different reduction potentials. In particular, selenium ($E^0_{Se^{4+}/Se^0} = 0.74V/NHE$) and copper ($E^0_{Cu^{2+}/Cu^0} = 0.342V/NHE$) have equilibrium potential more noble than indium ($E^0_{In^{3+}/In^0} = -0.338V/NHE$) and gallium ($E^0_{Ga^{3+}/Ga^0} = -0.523V/NHE$). The overall reaction leading to the deposition of stoichiometric CIGS is (Kaupmees, 2007):

$$1) \quad Cu^{2+} + In^{3+} + Ga^{3+} + 2SeO_3^{2-} + 12H^+ + 16e^- \rightarrow CuInGaSe_2 + 6H_2O$$

This reaction is the result of a combination of chemical and electrochemical reactions, but the exact mechanism is not well established because it depends on the redox potential of each species, solution composition and applied potential. There are two common hypotheses trying to explain the deposition of

CIGS. The first envisages formation of different copper-selenium phases, followed by incorporation of indium and gallium (Kaupmees, 2007). The other foresees the co-deposition of all selenium compounds (copper, indium and gallium selenides) because, according to the mechanism proposed by Kröger (Kröger, 1978), selenides deposition occurs at potentials more positive with respect to deposition of pure metals. Selenium compounds can either chemically or electrochemically react with each other, leading to the formation of CIS and CIGS phases. Whatever the mechanism, the electrodeposition of secondary phases is highly probable and then it is necessary to control different electrochemical parameters to limit the formation of a multiphase compound. In this work we have concentrated our attention on the optimization of applied potential, pH and composition of solution. As for the applied potential, we found that -1.15 V(SCE) is the best value to obtain a CIGS phase with a good stoichiometry. For applied potential below this value only CIS were deposited, whilst for values above -1.15V(SCE) very few changes in CIGS composition was recorded because of the simultaneous evolution of H_2. Solution pH is another parameter controlling the composition of deposit. In fact, in the case of films, a low pH favours the evolution of H_2, with a consequent low efficiency for CIGS deposition. For this reason, bath pH was adjusted to about 5 for films electrodeposition. Differently, in the case of NWs deposition the confining effect into alumina channels leads to an accumulation of OH^- ions (generated from the hydrogen reaction) at the electrode/electrolyte interface that progressively hinders H_2 evolution. Thus, for deposition of nanowires pH was that of the as-prepared solution without any adjustment (2.6).

Regarding solution composition, owing to the low redox potential for Ga deposition, it was necessary to operate with a higher Ga^{3+} concentration with respect to the other metals. In particular, solutions with a $Ga^{3+}/(Cu^{2+}+In^{3+})$ ratio in the range from 4 to 10 were used. Using these optimized parameters we have carried out depositions on electropolished Mo and into anodic alumina membranes. It is important to highlight that electropolishing was chosen as preliminary treatment of Mo sheets, because it ensures to obtain a very flat surface, taking into account that roughness influences the performance of CIGS electrodeposited films, as reported by NREL group (Basol, 2010). As for nanowires, these preliminary results were obtained on sputtered gold, but deposition on sputtered Mo is now in progress.

In all deposition conditions, the as-electrodeposited CIGS had amorphous structure, as expected on the basis of the literature (Lincot et all, 2004). An interesting result of the XRD analysis is the absence of any peak attributable to the metallic phases of four elements. This finding supports the conclusion that the four electrodeposited elements are mixed in a single phase. In order to obtain a crystalline deposit, thermal treatment was carried out in Ar atmosphere for 1h at 400°C. After this treatment a crystalline CIGS phase was detected by XRD analysis and identified with ICDD diffraction file no.35-1102. These films have a mean grain size (calculated by the Sherrer's equation) of about 20 nm.

In Table 1 is reported the mean composition of CIGS obtained at -1.15 V(SCE) for some samples. Films were obtained from a bath having a Ga/(Cu+In) molar ratio of 10. The variation of composition before and after thermal treatment is due to evaporation of Se during annealing. This result suggests that for obtaining an annealed CIGS with a good stoichiometry it is necessary to deposit a phase richer of Se. In the investigated conditions, as-prepared and annealed films are Cu-rich (Cu/In+Ga > 1). This is due to the formation of a highly conductive $Cu_{2-x}Se$ phase that was detected by micro-Raman spectroscopy. This analysis also showed that the presence of $Cu_{2-x}Se$ phase (whose mode is at about 260 cm^{-1}) decreases after thermal treatment, with the appearance of an additional mode, located at about 173 cm^{-1}, assigned to the CIGS phase. These results are in agreement with data reported in (Harati, 2010). The Cu_2Se phase was not detected by XRD analysis, also after the thermal treatment, and thus it is probably dispersed in the CIGS matrix. As reported in the literature (Basol, 2010), this phase can be eliminated performing a simple chemical etching of annealed samples in KCN solution.

Table 1. Mean composition of CIGS electrodeposits obtained at -1.15V(SCE).

Sample	Cu(at.%)	In(at.%)	Ga (at.%)	Se (at.%)	Cu/(In+Ga)	Ga/(In+Ga)
As Prepared Film	16.8	8.9	3.7	70.5	1.3	0.29
Film TT 1h at 400°C	36.4	18.4	8.4	36.8	1.36	0.31
As Prepared nanowires	20.3	15.0	13.1	51.3	0.72	0.47

In Figure 1, morphology of CIGS films before (Fig.1a) and after thermal treatment is shown. The as-deposited film appears not uniform with the surface covered by cauliflower-like florets of different size. For many authors, these cauliflower-like structures on the surface of the CIGS thin film consists principally of $Cu_{2-x}Se$ compounds (Lee et all, 2012). After annealing, samples displayed a more compact and uniform morphology (Fig.2a) and very few surface deposits are present. Besides, film is free from cracks and voids: this indicates a good adherence to the Mo substrate.

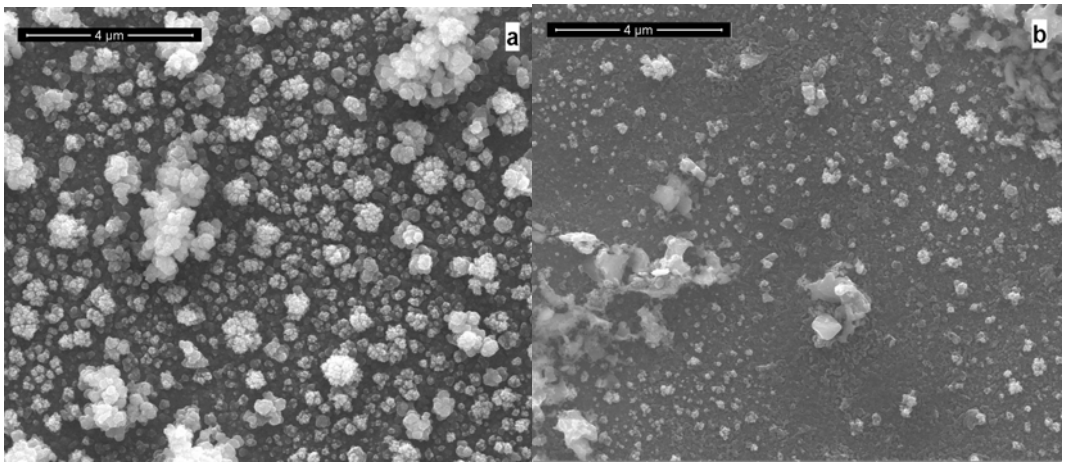

Figure 1: SEM images of CIGS films obtained by electrodeposition on electropolished Mo at -1.15 V(SCE) before (a) and after (b) annealing. Thermal treatment was carried out in argon atmosphere for 1h at 400°C.

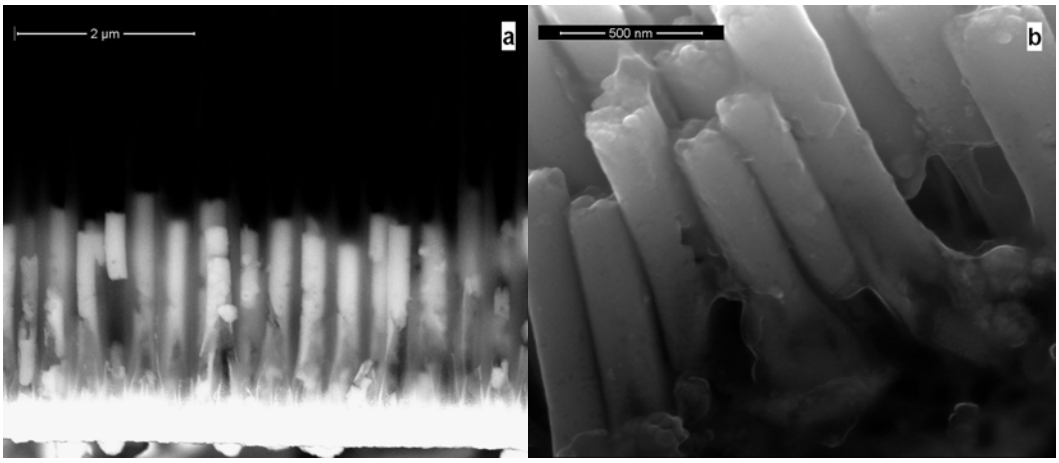

Figure 2: SEM images of CIGS nanowires obtained by electrodeposition inside the channels of alumina template at -1.15 V(SCE) before (a) and after (b) total dissolution of alumina membrane in 2 M H_3PO_4 solution. Image (a) was collected in BSE mode.

Morphology of the nanowires before and after total dissolution of the alumina template is shown in Figure 2. Fig. 2a shows that nanowires are uniformly distributed in all channels of the membrane: thus their density is of the order of 10^{13} NWs m^{-2}, equal to the pore population of the alumina template. Fig. 2b shows that NWs are straight with a cylindrical shape; their uniform diameter (about 210 nm) is almost equal to the size of the alumina channels, and the mean length is about 2 μm. Figure 2b is a backscattered electron image of the NWs array, revealing that they consist of a homogeneous phase. The composition of these nanowires is reported in Table 1; like for the case of films, they are amorphous. The Raman spectrum shows only a very broad and low mode at ~275 cm^{-1}, not easy to attribute. In some work it is claimed that also this mode is attributable to the $Cu_{2-x}Se$ phase (Xue et all, 2004). In any case, the very low intensity of this mode and its broadening allow to conclude that a more homogeneous composition was obtained in the case of electrodeposition of nanowires in comparison to films.

Both CIGS films and nanowires are photoactive, as revealed by the photocurrent investigation carried out in 0.1 M Na_2SO_4 aqueous solution. Figure 3 shows the photocurrent action spectra, corrected for the lamp photon emission, for the films of Table 1; spectra were recorded at the open circuit potential. For the annealed sample it is possible to observe a sharp decrease in photocurrent intensity, due to the change of CIGS composition. Shape of these spectra is quite different from that relative to nanowires, reported in (Inguanta, 2010a); in the latter case, spectrum presents two photocurrent peaks at around 450 and 560 nm, whose relative intensity changes with the experimental conditions. From photocurrent spectra we have estimated the optical gaps of CIGS deposits. Value of 1.55 and 1.7 eV have been estimated for the as-deposited NWs and film, respectively. For annealed films a value of 1.60 eV was obtained. In the case of as-deposited films, the optical gap was determined from the photocurrent onset wavelength, whilst for the

annealed film band gap was calculated by extrapolating to zero the plot of $(Iph\ h\nu)^2$ vs. $h\nu$, according to direct transitions. All the estimated gap values lie in the interval reported in the literature (Dharmadasa et all., 2007).

The p-type conductivity of the films was confirmed by recording the current transients, obtained chopping manually the light under continuous illumination (Figure 4). These last experiments evidence the presence of photocurrent spikes having the same sign of the pseudo-stationary response; after annealing spikes have a much lower intensity, maybe due to a decrease of the film defects.

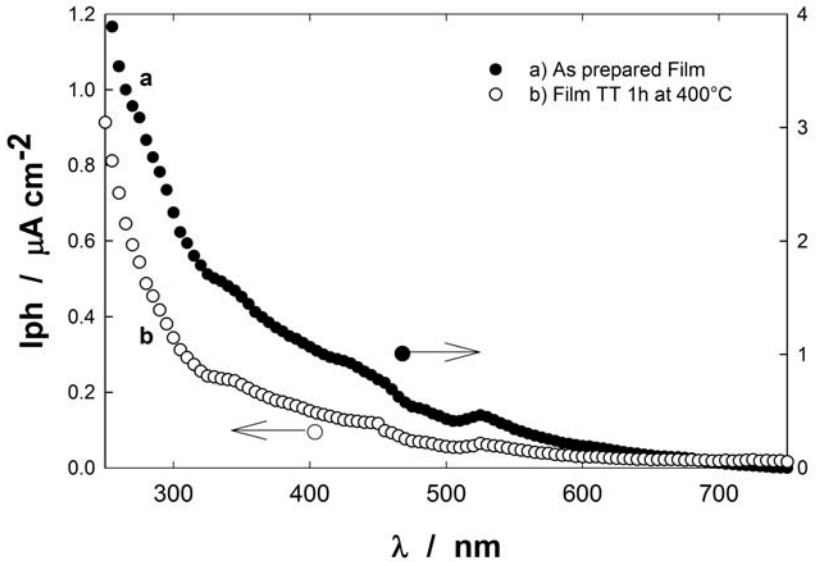

Figure 3: Photocurrent spectra of CIGS films obtained by electrodeposition on electropolished Mo at -1.15 V(SCE) before (a) and after (b) annealing. The spectrum of as-prepared CIGS NWs array is reported in (Inguanta et al. 2010a).

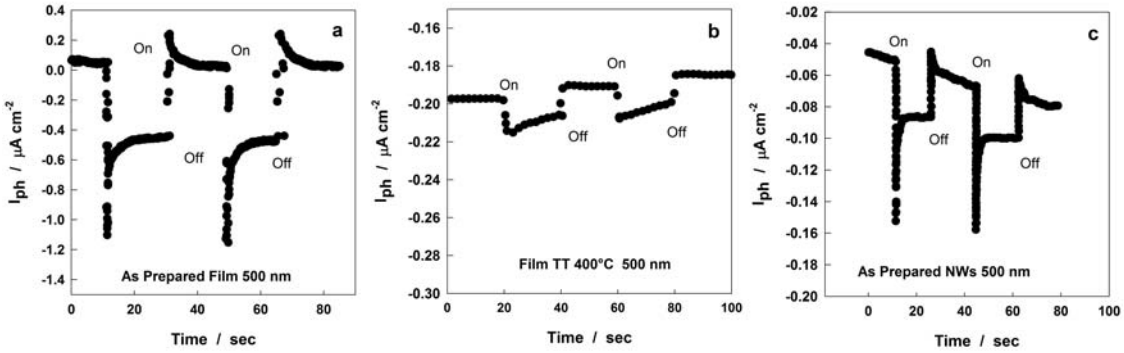

Figure 4: Current transients under monochromatic irradiation at 500 nm: (a) as-deposited CIGS film; (b) annealed CIGS film; (c) as-deposited CIGS NWs.

4. Conclusions

CIGS films and nanowires were fabricated successfully by a single-step electrochemical deposition at the applied potential of -1.15 V (SCE). The effect of metallic ion concentration in the electrolyte and bath pH on the composition of CIGS deposit was investigated. As-deposited films were also annealed at 400°C under Ar atmosphere for crystallization. The structural, morphological and compositional properties of the CIGS thin films before and after annealing were examined by XRD, SEM, EDS and Raman. We have shown that composition and crystalline structure of film change after thermal treatment. Annealing modify also morphology and photocurrent response of the deposit. Raman analysis revealed the presence of a $Cu_{2-x}Se$ phase, also before annealing. In the case of nanowires, a more homogenous amorphous CIGS phase was obtained; they present a perfectly cylindrical morphology with a uniform diameter throughout

length. Both films and nanowires were also characterized by photoelectrochemical measurements; all samples showed a cathodic photocurrent and gap values in the range of 1.55-1.7 eV.
Our approach suggests the possibility of large-scale production of CIGS solar cells via electrodeposition that could provide high quality CIGS with low capital investment because the use of low-cost starting materials, low deposition temperature and minimal waste generation (the solution can be recycled). Further investigations are in progress.

Acknowledgements.

This work was partially funded by the European Community through the “Programma Operativo Nazionale Ricerca e Competitività 2007-2013” (PON01_01725 Project).

References

Basol B. 2010, Commercialization of high efficiency low cost CIGS technology based on electroplating. Final Technical Progress Report.; NREL/SR-520-48590.

Dharmadasa IM., Chaure NB., Tolan GJ.,. Samantilleke AP. 2007. Development of p(+), p, i, n, and n(+)-type $CuInGaSe_2$ layers for applications in graded bandgap multilayer thin-film solar cells. J. Electrochem. Soc., 154, H466-H471

Harati M., Jia J., Giffard K., Pellarin K., Hewson C.,. Love DA., Ming Lau W., Ding Z. 2010. One-pot electrodeposition, characterization and photoactivity of stoichiometric copper indium gallium diselenide (CIGS) thin films for solar cells. Phys. Chem. Chem Phys. 12, 15282-15290.

Inguanta, R., Butera, M., Piazza, S., Sunseri, C. 2007, Fabrication of metal nano-structures using anodic alumina membranes grown in phosphoric acid solution: Tailoring template morphology, App. Surface Sci, 253, 5447-5456

Inguanta, R., Ferrara, G., Piazza, S., Sunseri, C. 2009. Nanostructures fabrication by template deposition into anodic alumina membranes. Chemical Engineering Transactions. 17, 957-962

Inguanta R., Livreri P., Piazza S., Sunseri C., 2010a, Fabrication and photoelectrochemical behavior of ordered CIGS nanowire arrays for application in solar cells., Electrochem. Solid State Lett. 13, K22-K25.

Inguanta R., Piazza S., Sunseri C., Cino A., Di Dio V., La Cascia D., Miceli R., Rando C., Zizzo G., 2010b, An electrochemical route towards the fabrication of nanostructured semiconductors solar cells”. In: Power Electronics, Electrical Drives, Automation and Motion, ISBN: 9781424449866. IEEE, 1166-1171.

Jackson P, Hariskos D, Lotter E, Paetel S., Wuerz R., Menner R., Wischmann, W., Powalla M., 2011, New world record efficiency for $Cu(In,Ga)Se_2$ thin-film solar cells beyond 20%. Prog. Photovoltaics, 19, 894–897.

Joint Committee Powder Diffraction Standards, Power Diffraction file. International Centre for Diffraction Data. Card 35-1102, Pennsylvania, 2007.

Kaupmees L., Altosaar M., Volubujeva O., Mellikov E., 2007, Study of composition reproducibility of electrochemically co-deposited $CuInSe_2$ films onto ITO. Thin Solid Films 515, 5891-5894

Kröger F. A., 1978, Cathodic Deposition and Characterization of Metallic or Semiconducting Binary Alloys or Compounds J.Electrochem. Soc. 125, 2028-2043

Lee H., Yoon H., Ji C., Lee D., Lee J-H., Yun J-H., Kim Y. 2012. Fabrication of CIGS Films by Electrodeposition Method for Photovoltaic Cells, 41, 3375-3381

D. Lincot, J. F. Guillemoles, S. Taunier, D. Guimard, J. Sicx-Kurdi, A. Chaumont, O. Roussel, O. Ramdani, C. Hubert, J. P. Fauvarque, et al., Sol. Energy, 77, 725 2004 .

Panthani M.G., Akhavan V., Goofellow B., Schmidtke J. P., Dunn L., Dodabalapur A., Barbara P. F., Korgel B. A., 2008, Synthesis of $CuInS_2$, $CuInSe_2$, and $Cu(In_xGa_{1-x})Se_2$ (CIGS) nanocrystal “inks” for printable photovoltaics., J Am. Chem. Soc. 130, 16770-16777.

Schultz O., Glunz S.W., Willeke G.P., 2004, , Prog. Photovoltaics, 12, 553-558.

Spanò T., Inguanta R., Livreri P., Piazza S., Sunseri C., 2012, Electrochemical deposition of CIGS on electropolished Mo, in Fuelling the Future: Advances in Science and Technologies for Energy Generation, Transmission and Storage. Editor A. Mendez-Villa, ISBN-13: 978-1-61233-558-2 BrownWalker Press,183-187.

Xue C.,. Papadimitriou D, Raptis Y.S., Richter W., Esser N., Siebentritt S., Lux-Steiner M.Ch. 2004. Micro-Raman Study of Orientation Effects of CuSe-Crystallites on Cu rich $CuGaSe_2$ Thin Films, Journal of Applied Physics, 96, 1963-1966